Analysis of Large Planar Arrays of Single-Wall Carbon Nanotubes

George W. Hanson, *Fellow, IEEE*, Steffen McKernan, and Dawei Wang

***Abstract*—Electromagnetic properties of finite planar arrays of infinite-length single-wall carbon nanotubes are determined. A modal capacitance and inductance is identified and the nanotube-to-ground-plane total capacitance is obtained using two methods, one based on the total capacitance matrix and the other on a dynamic modal method. Both methods incorporate the quantum capacitance in a natural manner. The formulation proceeds from Boltzmann's equation and Maxwell's equations and does not require as an initial assumption an equivalent transmission line model. Good agreement is shown with measured results.**

***Index Terms*—Carbon nanotubes, multiconductor transmission lines, nanotechnology.**

I. Introduction

MASSIVELY parallel planar arrays of single-wall carbon nanotubes (SWCNTs) consisting of thousands of individual tubes are of interest as interconnects and in devices. In many applications, one would like to replace a single bulk conductor with a carbon nanotube because of the highly desirable mechanical and electrical properties of carbon nanotubes [1] (high mechanical strength and stiffness, high thermal conductivity, tolerance of extreme heating and large current carrying capability, resistance to electromigration, tunability, etc.). In fact, SWCNTs can support current densities up to 10^9 A/cm^2 without melting [2], significantly larger than traditional metals, which typically have maximum current densities on the order of $10^5 - 10^6$ A/cm^2. The impressive characteristics of SWCNTs are partly due to intrinsic material properties associated with the carbon–carbon bond, but also due to the fact that carbon nanotubes can be fabricated as 1-D conductors with very few defects. In comparison, typical nanowires suffer from surface and grain-boundary scattering, electromigration [3], and for some materials such as copper, oxidation [4].

However, in comparison with larger radius metal nanowires, an individual carbon nanotube has a large contact resistance, and beyond the ballistic transport regime, an ohmic resistance that is too large to be practical in many applications, although the scaled nanotube contact and channel resistances are extremely low in comparison to bulk semiconductors. The actual current on a nanotube is limited to approximately 25 μA by its extremely small cross section and many applications (e.g., RF amplifiers) require much larger currents. Therefore, a large collection of carbon nanotubes in a bundle or array configuration (effectively acting in parallel) are attractive to satisfy low impedance and/or sufficiently large current requirements, while still exhibiting many of the unique properties of the nanotubes themselves.

In this study, finite, but large planar arrays of infinite-length SWCNTs over a perfect ground plane are considered; the same analysis applies to a two-row structure without a ground plane carrying a propagation mode having odd vertical symmetry (i.e., the usual transmission line mode). The effects of ground-plane finite conductivity are not considered and would necessitate a Sommerfeld treatment or other analysis [5]; in particular, a finitely conducting ground plane can affect inductance calculation, but will have a minimal effect on capacitance determination, which is a major aspect of this study. The case when all nanotubes are held at a common potential (by, say, depositing an electrode across each end of all tubes in the array) is of particular interest for applications that essentially replace a single conductor with an array of nanotubes. We are then interested in the total capacitance seen from the nanotube array to the ground plane, which we call C_{array} and the inductance of the array, L_{array}. In particular, C_{array} is important in carbon-nanotube transistor design. Two formulations of C_{array} are provided, one based on the total capacitance matrix and the other on modal dynamics, with good agreement between the two methods. Related capacitance calculations for an infinite array appear in [6] and for a finite array in [7]. The electrodynamic formulation presented here, based on Boltzmann/Maxwell's equations, is quite different from previous work and naturally accommodates the quantum capacitance without the need for a transmission line model or energy considerations. The analysis proceeds from the general formulation presented in [8].

In the following, we consider infinitely long tubes and determine per-unit-length capacitance and inductance quantities. The results apply to finite-length nanotubes that are sufficiently long so that the basic physical processes governing transport are length independent. That is, the tubes should be longer than the electronic length scales λ_F, the Fermi wavelength, and L_{mfp}, the mean-free path. The former would lead to quantization in the axial direction, which would occur for extremely short tubes (approximately less than 10 nm in length). The latter governs

Manuscript received November 18, 2010; revised April 12, 2011; accepted April 30, 2011. Date of publication June 16, 2011; date of current version October 12, 2011.

G. W. Hanson is with the Department of Electrical Engineering, University of Wisconsin–Milwaukee, Milwaukee, WI 53211 USA (e-mail: george@uwm.edu).

S. McKernan resides in San Clemente, CA 92672 USA (e-mail: Steffen_McKernan@yahoo.com).

D. Wang is with the RF Nano Corporation, Newport Beach, CA 92660 USA (e-mail: Dawei.Wang@rfnano.com).

Color versions of one or more of the figures in this paper are available online at http://ieeexplore.ieee.org.

Digital Object Identifier 10.1109/TMTT.2011.2156422

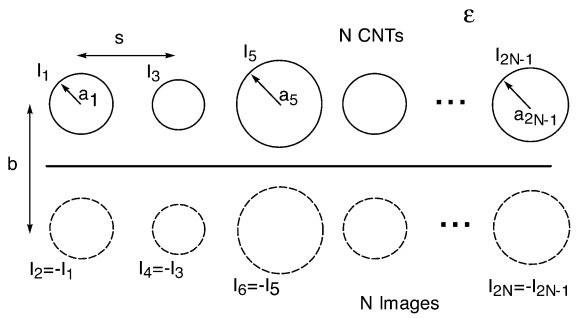

Fig. 1. Array of N SWCNTs above a ground plane, modeled using image theory as an array of $2N$ tubes in a homogeneous space. Current on the nth tube is indicated as I_n.

the change over from ballistic transport to diffusive transport as nanotube length becomes greater than L_{mfp}. In this work, for resistance calculations, we consider tubes in the diffuse transport regime, although for capacitance and inductance calculations, the results are independent of the mean-free path and are valid in the ballistic transport regime as well. Throughout the paper, SI units are used and the (suppressed) time dependence is $e^{j\omega t}$.

II. Analysis of a Planar Array of SWCNTs

Our interest is in obtaining the modal properties and total array resistance, capacitance and inductance for a planar array of SWCNTs over a ground plane, as depicted in Fig. 1, where the z-axis is into the page. For the nth tube, the radius is a_n, the conductivity is σ_n, b is the distance between rows of tubes (i.e., $b/2$ is the distance to the ground plane), and the center-to-center horizontal spacing between tubes is s.

One method of analysis would be to extend the multiconductor transmission line model, which is well known for macroradius conductors [9], to nanoradius conductors. The extension would need to incorporate the kinetic inductance and quantum capacitance of nanoradius conductors, similar to what was done for the two-conductor carbon-nanotube transmission line in [10]. Rather than follow this approach, which would require as a starting point an assumed transmission line circuit model, here we start with a Maxwell equation/Boltzmann equation model and derive all modal properties and capacitance and inductance values from rigorous coupled integral equations.

We consider the case of N nanotubes above a ground plane (i.e., N nanotubes and N image tubes), but the same analysis holds for a two-row structure having $2N$ nanotubes without a ground plane carrying a propagation mode having odd vertical symmetry. The analysis starts with the integral equation for a single carbon nanotube [8, eq. (7)]

$$\left(k^2+\frac{\partial^2}{\partial z^2}\right)\int K(z-z')\,I(z')dz' = \frac{j\omega\varepsilon}{a\sigma(\omega)}\left(1+\xi\frac{\partial^2}{\partial z^2}\right)I(z)-j2\pi\omega\varepsilon E_z^i(z) \quad (1)$$

where $I(z)$ is the current on the nanotube, $K(z-z') = \int_{-\pi}^{\pi} d\phi' e^{-jkR}/4\pi R$ is the kernel, $k^2 = \omega^2\mu_0\varepsilon$ is the wavenumber in the homogeneous dielectric, a is nanotube radius, E_z^i is an impressed electric field, and

$$\sigma(\omega) = \frac{-j2e^2v_F}{\hbar\pi^2 a(\omega - i\tau^{-1})} \quad (2)$$

$$\xi = \frac{jv_F^2\tau}{\omega(1+j\omega\tau)} \quad (3)$$

are the conductivity and spatial dispersion parameter, respectively, for the metallic nanotube, with v_F being the electron Fermi velocity and τ being the momentum relaxation constant. The spatial dispersion parameter (3) was derived in [8] and differs slightly from the quantity presented in [11]; this new expression arises from a number-conserving solution of Boltzmann's equation and provides the correct expression for quantum capacitance $C_q = 8e^2/hv_F$ and leads to $L_kC_q = 1/v_F^2$, where $L_k = h/8e^2v_F$ is the kinetic inductance, as discussed in [8, Appendix]. The conductivity (2) is valid for small radius metallic tubes consisting of two electron channels. For larger radius tubes with more than two conducting channels, (2) is multiplied by $M/2$, where M is the number of conducting channels [12]. In the following, we use $M = 2$, but the subsequent results can easily be modified by including the factor M in (5) below. Semiconducting tubes can be accommodated by replacing (2)–(3) with the values for a semiconducting tube, which need to be found numerically [11].

Starting from (1), the system of equations describing an array of nanotubes, as depicted in Fig. 1, is [8, eq. (63)]

$$I_n\left(\ln\left(\frac{b}{a_n}\right)-Q_n\right) + \sum_{m=1,3,5,\ldots,m\neq n}^{2N} I_m\ln\left(\frac{b_{n,m+1}}{b_{n,m}}\right) = -2\pi j\omega\varepsilon E^i_{z,\text{tube }n} \quad (4)$$

for $n = 1,3,5,\ldots,2N$, where b_{nm} is the center-to-center distance between nanotubes n and m and where

$$Q_n = \frac{j\omega\varepsilon\left(1-\xi_n\beta^2\right)}{(k^2-\beta^2)\,a_n\sigma_n} = \frac{j\omega 2\pi\varepsilon}{(k^2-\beta^2)}\left(R_{cn,n}+j\omega L_k+\frac{\beta^2}{j\omega C_q}\right) \quad (5)$$

contains all information about the nanotube's material properties with $R_{cn,n} = h/8e^2v_F\tau$ being the resistance of the nth carbon nanotube ($\tau = \tau_n$ depends on tube chirality; if we approximate τ as being constant, then $Q_n = Q$ is independent of nanotube number), L_k and C_q are the kinetic inductance and quantum capacitance introduced previously, I_n is the current on the nth tube, and β is the axial wavenumber such that $I_n(z) = I_ne^{-j\beta z}$.

In matrix form, (4) can be written as

$$\mathbf{M}(\beta)\,\mathbf{I} = [\mathbf{P} - \mathbf{Q}(\beta)]\,\mathbf{I} = \mathbf{F} \tag{6}$$

where $\mathbf{M}$, $\mathbf{P}$, and Q are $N \times N$ matrices (Q is a diagonal matrix with entries $Q_{nn} = Q_n$), $\mathbf{I}$ is an $N \times 1$ column of unknown current amplitudes, and $\mathbf{F}$ is an $N \times 1$ excitation column. Propagation constants β can be determined from $|\mathbf{M}(\beta)| = 0$ (see [8, eq. (67)] for the $N = 1$ two-nanotube case), leading to the $\boldsymbol{\alpha}$th propagation mode. The matrix $\mathbf{P}$ is independent of β, frequency, and material parameters and only depends on the geometry of the array.

At this point, we could solve the forced problem, determine the induced transform domain currents $\mathbf{I}(\beta) = \mathbf{M}^{-1}(\beta)\,\mathbf{F}$, and invert the current on each nanotube into the space domain via

$$\mathbf{I}(z) = \frac{1}{2\pi}\int_{-\infty}^{\infty} \mathbf{I}(\beta)\, e^{j\beta z} d\beta. \tag{7}$$

However, here we are interested in the modal propagation constants and so we solve the unforced problem (setting $E_z^i = 0$, $\mathbf{F} = \mathbf{0}$). The propagation constants are determined as the complex values $\beta = \beta_p$ that force $|\mathbf{M}(\beta_p)| = 0$. The null space of the matrix evaluated where $|\mathbf{M}(\beta_p)| = 0$ leads to the modal currents I_1, I_2, I_N (equivalently, we can determine the eigenvectors of $\mathbf{M}(\beta)$ associated with a zero eigenvalue). We can write the resulting null space amplitudes as $I_n = I_n^p,\ n = 1,2,\ldots N$, leading to N different current values for every mode p.

Since $\mathbf{Q}$ is a diagonal matrix, if $Q_n = Q$ for all n (i.e., identical nanotubes or ignoring the chirality dependence of τ), we can write

$$[\mathbf{M}(\beta)] = [\mathbf{P}(\beta) - Q(\beta)\,\mathbf{1}] \tag{8}$$

where Q is the scalar function (5) and $\mathbf{1}$ is the identity matrix. Although the root β_p that forces $|\mathbf{M}(\beta_p)| = 0$ depends on Q (and, hence, on the resistance, kinetic inductance, and quantum capacitance of the nanotubes), by a well-known theorem in linear algebra, the eigenvectors of $[\mathbf{M}(\beta)]$ are the same as the eigenvectors of $[\mathbf{P}(\beta)]$ for any given β, in which case the modal current amplitudes values (eigenvectors) are independent of the (identical) nanotube's material properties and frequency and only depend on the array geometry (i.e., on s and b) for a given mode.

As an explicit example, for $N = 3$ and relabeling the conductors, as shown in Fig. 2, we have

$$\mathbf{P} = \begin{bmatrix} \ln\left(\frac{b}{a_{-1}}\right) & \ln\left(\frac{d_1}{s}\right) & \ln\left(\frac{d_2}{2s}\right) \\ \ln\left(\frac{d_1}{s}\right) & \ln\left(\frac{b}{a_0}\right) & \ln\left(\frac{d_1}{s}\right) \\ \ln\left(\frac{d_2}{2s}\right) & \ln\left(\frac{d_1}{s}\right) & \ln\left(\frac{b}{a_1}\right) \end{bmatrix} \tag{9}$$

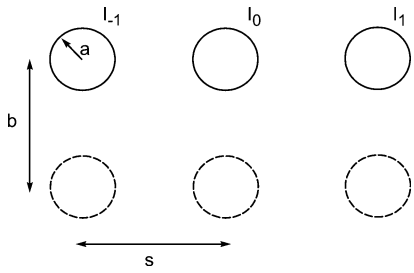

Fig. 2. $N = 3$ nanotube case with currents labeled from the center outwards.

where $d_n = \sqrt{(ns)^2 + b^2}$, which, with $\mathbf{L} = \mu/\pi\mathbf{P}$, leads to the inductance matrix in [9, Sec. 3.2.3.2] and $\mathbf{C} = \pi\varepsilon\mathbf{P}^{-1}$. This results in a capacitance matrix consistent with the system

$$\begin{bmatrix} q_1 \\ q_2 \\ q_3 \end{bmatrix} = \begin{bmatrix} C_{11} & C_{12} & C_{13} \\ C_{21} & C_{22} & C_{23} \\ C_{31} & C_{32} & C_{33} \end{bmatrix} \begin{bmatrix} \phi_1 \\ \phi_2 \\ \phi_3 \end{bmatrix} \tag{10}$$

where C_{ij} is the ratio of charge on nanotube i due to voltage ϕ_j on nanotube j with all other voltages set to zero.

As shown in [8, eq. (71)], (6) can be written as

$$\left[\omega^2(\mathbf{L} + \mathbf{L}_k) - \beta^2\left(\mathbf{C}^{-1} + \mathbf{C}_q^{-1}\right) - j\omega\mathbf{R}\right]\mathbf{I} = \frac{\left(k^2 - \beta^2\right)}{\varepsilon\pi}\mathbf{F} \tag{11}$$

where $\mathbf{R}$, $\mathbf{C}_q$, and $\mathbf{L}_k$ are diagonal matrices with $\mathbf{L}_k = 2L_k\mathbf{1}$, $\mathbf{C}_q = (C_q/2)\,\mathbf{1}$, and the ohmic resistance diagonal matrix $\mathbf{R}$ has entries $2R_{cn,n}$ (all matrices are per-unit-length quantities). This result is for two rows of nanotubes having currents with odd symmetry in the vertical direction and so the factors of 2 reflect the presence of two conductors. In the Appendix, the capacitance result is derived via a Thomas–Fermi model as an alternative method. For conductors above a perfect ground plane, we would divide (11) by 2 to account for the presence of the ground plane (in which case the return row of conductors (i.e., images) does not exhibit R_{cn}, L_k, and C_q and the geometric capacitance and inductance is modified by the ground plane (see the discussion in [8, eq. (72)]).

III. Total Array-to-Ground Capacitance and Array Inductance

In applications where a carbon-nanotube array is used as a replacement for a single conductor (or channel in a device), we are interested in the situation where we hold all nanotubes at a common potential by using an electrode at each end of the array, as depicted in Fig. 3 (we assume that the electrode is thin, and other than holding the nanotubes at the same potential, plays no role). We are then interested in the total capacitance seen from the nanotube array to the ground plane C_{array} and the inductance of the array L_{array}. In this case, we view the nanotube array as a conducting system along which one or more transmission line modes can propagate. In the following, we will develop two different forms for C_{array}, which we will call $C_{\text{array}}^{(1)}$ and $C_{\text{array}}^{(2)}$.

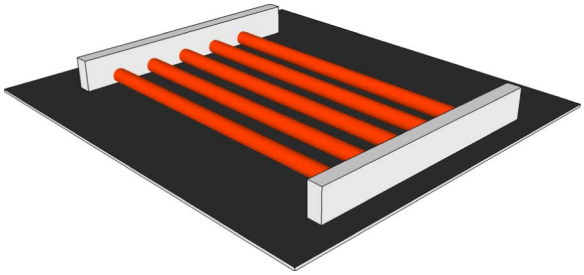

Fig. 3. Carbon-nanotube array used as a replacement for a single conductor or as a channel in a device. The array is over a ground plane and the tubes are connected at each end by electrodes (positioned above the ground plane).

One typical method to determine the capacitance of a two-conductor system is to apply a static (dc) voltage ϕ due to a voltage source across the conductors and determine the resulting charge $\pm Q_T$ using some method, the ratio Q_T/ϕ being the capacitance. Another method is to assume a static charge $\pm Q_T$ on the conductors and determine the static voltage ϕ produced by this charge, the ratio being the capacitance. However, neither method would incorporate the quantum capacitance of the elements comprising the structure. The quantum capacitance results from the carbon nanotube's finite density of states and the total capacitance does not arise from the electrostatic potential, but from the electrochemical potential. The electrochemical potential energy is [13]

$$\mu_e = \mu - e\phi \tag{12}$$

where μ is the chemical potential energy. The total array capacitance is

$$C_{\text{array}} = -e\frac{Q_T}{\mu_e}. \tag{13}$$

A. $C^{(1)}_{\text{array}}$: Static Array Capacitance and Inductance

One method to obtain C_{array} is to identify the total capacitance from (11) as

$$\mathbf{C}^T = \left(\mathbf{C}^{-1} + \mathbf{C}_q^{-1}\right)^{-1} = \left(\frac{1}{\pi\varepsilon}\mathbf{P} + \mathbf{C}_q^{-1}\right)^{-1}. \tag{14}$$

Rather than (10), $\mathbf{Q} = \mathbf{C}\phi$, the correct charge-electrochemical potential matrix relationship is

$$\mathbf{Q} = \mathbf{C}^T\boldsymbol{\mu}_e \tag{15}$$

where $\boldsymbol{\mu}_e$ is the electrochemical potential (not electrochemical potential energy) matrix. If we define the capacitance C_{array} as the ratio of the sum of all charge on all nanotubes ($Q_T = q_1+q_2+q_3+\cdots+q_N$) to the common electrochemical potential on all nanotubes, then

$$C^{(1)}_{\text{array}} = \sum_{n=1}^{N}\sum_{m=1}^{N} C^T_{n,m}. \tag{16}$$

That is, $C^{(1)}_{\text{array}}$ is the sum of all matrix entries in the total capacitance matrix. For an array of tubes over a ground plane, we multiply each capacitance entry by 2. The units of capacitance are Farads/meter.

By taking $C_q \to \infty$ to implement the infinite density of states result, we obtain the usual electrostatic capacitance $C_{es,\text{array}}$ as the ratio of the sum of all charge on all nanotubes to the common electrostatic potential, which, from $\mathbf{Q} = \mathbf{C}\phi$, leads to

$$C_{es,\text{array}} = \sum_{n=1}^{N}\sum_{m=1}^{N} C_{n,m}. \tag{17}$$

The magnetostatic array inductance can be obtained as $L_{es,\text{array}} = \mu\varepsilon\left(C_{es,\text{array}}\right)^{-1}$ and the total array inductance (including kinetic inductance) as $L^{(1)}_{\text{array}} = L_{es,\text{array}} + L_k/N$. The expression (16) and that for $L^{(1)}_{\text{array}}$ are independent of τ and thus apply to both the diffusive and ballistic transport regimes.

B. $C^{(2)}_{\text{array}}$: Modal Array Capacitance and Inductance

As another method of determining capacitance, for each nanotube n we can define a dynamic modal capacitance $C_n^{\boldsymbol{\alpha},\text{dyn}}$ as being equal to $-e$ times the ratio of the change in charge $\delta q_n^{\boldsymbol{\alpha}}$ on the nanotube for a given propagation mode $\boldsymbol{\alpha}$ (i.e., at a value of propagation constant β such that $|\mathbf{M}(\beta)| = 0$, leading to the current amplitude null space vector $\mathbf{I}^{\boldsymbol{\alpha}}$) to the change in electrochemical potential $\delta\mu_e$ associated with introducing that charge,

$$C_n^{\boldsymbol{\alpha},\text{dyn}} = -e\frac{\delta q_n^{\boldsymbol{\alpha}}}{\delta\mu_e}. \tag{18}$$

The superscript $\boldsymbol{\alpha}$ indicates that the value of capacitance depends on the mode in question. Since we have a parallel collection of nanotubes, the total capacitance of the array is

$$C^{(2)}_{\text{array}} = C^{\boldsymbol{\alpha},\text{dyn}}_{\text{array}} = NC_n^{\boldsymbol{\alpha},\text{dyn}}\ \text{F/m}. \tag{19}$$

To determine this capacitance, we start with the space-domain modal current on the nth nanotube in the array,

$$I_n^{\boldsymbol{\alpha}}(z) = A_n^{\boldsymbol{\alpha}}e^{j\beta z} \tag{20}$$

where amplitudes A_n^{α} are determined from the null space of (6) [equivalently, (11)]. The determination of the modal linear charge density (C/m) on nanotube n is now straightforward,

$$\delta q_n^{\boldsymbol{\alpha}} = -\frac{1}{j\omega}\frac{dI_n^{\boldsymbol{\alpha}}(z)}{dz} = -\frac{1}{j\omega}j\beta A_n^{\boldsymbol{\alpha}}e^{j\beta z}. \tag{21}$$

We assume thermal equilibrium and quasi-static variation so that the electrochemical potential on each tube must be constant,

$$\mu_e = \mu(z) - e\phi(z) = \text{const} \tag{22}$$

where μ is the chemical potential. Now consider the difference between the tubes carrying a modal charge and the charge-free

tubes. For the charge-free tubes, each nanotube is neutral, $\mu = \mu^0$ and $\phi = \phi^0$ are constant, and $\mu_e = \mu_e^0$. Upon inducing a modal charge configuration on the tubes, we have an electron charge per unit length δq on each tube, which will induce a uniform shift $\delta\mu_e$ in the electrochemical potential from the former value μ_e^0. In general, we will have a nonuniform charge distribution and thus we expect both the chemical potential and electrostatic potential to be nonuniform, $\mu = \mu^1(z)$ and $\phi = \phi^1(z)$, but with the same axial dependence. Let $\delta\mu(z) = \mu^1(z) - \mu^0$ and $\delta\phi(z) = \phi^1(z) - \phi^0$. The electrochemical potential is constant at $\mu_e^1 = \mu_e^0 + \delta\mu_e$ and we have

$$\delta\mu_e = \mu_e^1 - \mu_e^0 = \delta u(z) - e\delta\phi(z). \tag{23}$$

We will assume that the chemical potential depends only on the local number density $n(z)$ of free carriers. In a linear approximation,

$$\delta\mu(z) = \left.\frac{\partial\mu}{\partial n}\right|_{n=n^0} \delta n(z) \tag{24}$$

where δn is the shift in electron number density.

The local electron surface charge density ($\mathrm{C/m^2}$) is

$$\rho_s(z) = -e\delta n(z) = -e\frac{\delta\mu(z)}{\left.\frac{\partial\mu}{\partial n}\right|_{n=n^0}} = \frac{\delta q_n^{\boldsymbol{\alpha}}}{2\pi a} \tag{25}$$

where we can define

$$l_s = \frac{\varepsilon}{e^2}\left.\frac{\partial\mu}{\partial n}\right|_{n=n^0} \tag{26}$$

as the screening length (meters), leading to the screening wavenumber $k_s = l_s^{-1}$. For a carbon nanotube [14],

$$k_s a = \frac{C_q}{2\pi\varepsilon} \tag{27}$$

The voltage between the nanotube at $r = 0$ and the ground plane is 1/2 the voltage from the tube to its image at $r = b$,

$$\phi_{\mathrm{tube-image}}^{\boldsymbol{\alpha}} = -\frac{1}{2}\int_{-b}^{0} 2E_r^{\boldsymbol{\alpha},T}(\mathbf{r})\,dr \tag{28}$$

where $E_r^{\boldsymbol{\alpha},T}$ is the total radial electric field due to current on all nanotubes. The radial electric field due to current on nanotube n is

$$E_r^{\boldsymbol{\alpha},(n)}(\mathbf{r}) = \frac{1}{j\omega\varepsilon}\left(\frac{\partial}{\partial r}\frac{\partial}{\partial z}\int_{-\infty}^{\infty}\int_{-\pi}^{\pi}\frac{e^{-jkR}}{4\pi R}\frac{I_n^{\boldsymbol{\alpha}}(z')}{2\pi}d\phi' dz'\right). \tag{29}$$

The voltage from nanotube n to ground is then

$$\delta\phi = \delta\phi_n^{\boldsymbol{\alpha}} = \frac{A_n^{\boldsymbol{\alpha}} j\beta e^{j\beta z}}{-j4\pi\omega\varepsilon}\frac{2}{2\pi} \times\left(\ln\left(\frac{b}{a}\right) + 2\sum_{m=1}^{N-1/2}\frac{A_m^{\boldsymbol{\alpha}}}{A_0^{\boldsymbol{\alpha}}}\ln\left(\frac{d_m}{ms}\right)\right) \tag{30}$$

and therefore, the dynamic capacitance from nanotube n to ground (yet in the presence of the other nanotubes) is

$$C_n^{\boldsymbol{\alpha},\mathrm{dyn}} = -e\frac{\delta q_n^{\boldsymbol{\alpha}}}{\delta\mu_e} = -e\frac{-\frac{1}{j\omega}j\beta A_n^{\boldsymbol{\alpha}} e^{j\beta z}}{\left.\frac{\partial\mu}{\partial n}\right|_{n=n^0}\delta n(z) - e\delta\phi_n^{\boldsymbol{\alpha}}(z)} \tag{31}$$

$$= \frac{2\pi\varepsilon}{\frac{2\pi\varepsilon}{C_q} + \left(\ln\left(\frac{b}{a}\right) + 2\sum_{m=1}^{N-1/2}\frac{A_m^{\boldsymbol{\alpha}}}{A_0^{\boldsymbol{\alpha}}}\ln\left(\frac{d_m}{ms}\right)\right)}. \tag{32}$$

Since $C_n^{\boldsymbol{\alpha},\mathrm{dyn}}$ is independent of n, for a given mode $\boldsymbol{\alpha}$, the capacitance of each nanotube to ground is the same. Finally, we obtain $C_{\mathrm{array}}^{(2)}$ from (19).

Note that (32) is the same result as would be obtained by combining the infinite density of states result (setting $l_s = 0$, or $C_q \to \infty$)

$$C_{es}^{\boldsymbol{\alpha},\mathrm{dyn}} = \frac{\delta q_n^{\boldsymbol{\alpha}}}{\delta\phi} = \frac{2\pi\varepsilon}{\left(\ln\left(\frac{b}{a}\right) + 2\sum_{m=1}^{N-1/2}\frac{A_m^{\boldsymbol{\alpha}}}{A_0^{\boldsymbol{\alpha}}}\ln\left(\frac{d_m}{ms}\right)\right)} = C_{es}^{\boldsymbol{\alpha}} \tag{33}$$

in series with C_q.

We refer to $C_{es}^{\boldsymbol{\alpha}}$ as the modal capacitance. The corresponding inductance can be obtained as $L_{es}^{\boldsymbol{\alpha}} = \mu\varepsilon/C_{es}^{\boldsymbol{\alpha}}$,

$$L_{es}^{\boldsymbol{\alpha}} = \frac{\mu}{2\pi}\left(\ln\left(\frac{b}{a}\right) + 2\sum_{m=1}^{N-1/2}A_m^{\boldsymbol{\alpha}}\ln\left(\frac{d_m}{ms}\right)\right). \tag{34}$$

For $s \to \infty$, $(d_m/ms) \to 1$, and

$$L_{es}^{\boldsymbol{\alpha}} = L_{es} = \frac{\mu}{2\pi}\ln\left(\frac{b}{a}\right) \tag{35}$$

$$C_{es}^{\boldsymbol{\alpha}} = C_{es} = \frac{2\pi\varepsilon}{\ln\left(\frac{b}{a}\right)} \tag{36}$$

the usual formulas for a wire above a ground plane, as expected.

The array inductance is

$$L_{\mathrm{array}}^{(2)} = L_{\mathrm{array}}^{\boldsymbol{\alpha},\mathrm{dyn}} = \frac{L_{cn} + L_{es}^{\boldsymbol{\alpha}}}{N}\ \mathrm{H/m}. \tag{37}$$

Similarly, for array resistance

$$R_{\text{array}} = \frac{R_{cn}}{N}\ \Omega/\text{m} \tag{38}$$

which is mode independent. For a finite-length array of carbon nanotubes, we need to include the contact resistance R_c (Ω). Assuming nanotube length l, this leads to

$$R_{\text{array}} = \frac{R_{cn}l + 2R_c}{N}\ \Omega. \tag{39}$$

Experiments in [15] show that for a massively parallel array, $R_{\text{array}} \simeq 50\ \Omega$ can be achieved. For example, consider a situation similar to the experimental setup of [15] with tube length $l = 1\ \mu$m, $N = 1000$ nanotubes and nanotube density of 10 NT/μm. In the experiment, there was no ground plane, thus we can ignore the capacitance. Then $R_{\text{array}} \simeq 20\ \Omega$, $L_{\text{array}} = 3.4$ pH, and thus the array impedance at 10 GHz is $Z_{\text{array}} \simeq 20 + j0.2\ \Omega$. This is consistent with measurements that showed that the real part varied from a few ohms to several tens of ohms for different samples and that the imaginary part was $0 \pm 10\ \Omega$ (the correspondence with $R_{cn}l/\text{NT}$ and $L_{cn}l/\text{NT}$ was discussed in [15]).

C. Interpretation of $C_{\text{array}}^{\boldsymbol{\alpha},\text{dyn}}$ and $L_{\text{array}}^{\boldsymbol{\alpha},\text{dyn}}$: Modal Patterns and Excitation of Modes

We now have array capacitance computed using two different methods, leading to $C_{\text{array}}^{(1)}$ and $C_{\text{array}}^{(2)}$ ($= C_{\text{array}}^{\boldsymbol{\alpha},\text{dyn}}$). There remains a question as to in what way will these quantities predict the actual quantities measured for a given structure (e.g., extracted from S-parameter data for an electrode connected array). To answer this question, we need to consider the possible modes of the structure and the size of the array.

We can obtain all possible modes by setting the forcing term in (6) to zero and performing a root search for complex β values such that $|\mathbf{M}(\beta_p)| = 0$. For two nanotubes ($N = 2$), we obtain the usual even and odd modes, where currents are in the same and opposite directions, respectively, on the nanotubes. In this case, we obtain

$$L_{\text{array}}^{\alpha,\text{dyn}} = L_{cn} + \frac{\mu}{2\pi}\left(\ln\left(\frac{b}{a}\right) \pm \ln\left(\frac{d_1}{s}\right)\right) \tag{40}$$

for the even and odd mode, respectively, which is the usual result and we find that $C_{\text{array}}^{(1)} = C_{\text{array}}^{(2)}$ and $L_{\text{array}}^{(1)} = L_{\text{array}}^{(2)}$ (i.e., the two methods, static and dynamic, yield identical results) for the even mode; the static values are based on summing all charges, and thus this only yields a nonzero result for the even mode). However, for $N \geq 3$, there is no similar mode having equal magnitude currents (e.g., where $A_n^{\boldsymbol{\alpha}} = 1$ for all n).

As an example, for one nanotube in air over a ground plane, with $b = 20$ nm, $f = 1$ GHz, and $a = 0.8814$ nm (which corresponds to a $(13,13)$ nanotube), the propagation value is found to be $\beta_p/k = 931.48 - j928.73$. For $N = 2$, identical nanotubes above a ground plane having $s = 10$ nm, using the two eigenvalues λ_n of the 2×2 matrix $\mathbf{P}$ and [8, eq. (66)], we obtain $\beta_e/k = 830.58 - j828.1$ for the even mode and $\beta_o/k = 1081.2 - j1078.1$ for the odd mode with the normalized eigenvectors being

$$\mathbf{I}_e = \begin{bmatrix} 1 \\ 1 \end{bmatrix} \quad \mathbf{I}_o = \begin{bmatrix} 1 \\ -1 \end{bmatrix}. \tag{41}$$

The values $\beta_{e/o}$ are dependent on frequency, geometric, and material properties of the array, but $\mathbf{I}_{e/o}$ only depend on the array geometry (i.e., b, a, s, and N).

For $N = 3$, we obtain three fundamental propagation modes associated with the three eigenvalues of $\mathbf{P}$, $\beta_1/k = 780.54 - j778.19$, $\beta_2/k = 987.91 - j985.02$, and $\beta_3/k = 1124 - j1120.7$. The modal current distributions/eigenvectors of $\mathbf{P}$ are

$$\mathbf{I}_1 = \begin{bmatrix} 0.823 \\ 1 \\ 0.823 \end{bmatrix} \quad \mathbf{I}_2 = \begin{bmatrix} -1 \\ 0 \\ 1 \end{bmatrix} \quad \mathbf{I}_3 = \begin{bmatrix} -0.608 \\ 1 \\ -0.608 \end{bmatrix} \tag{42}$$

(again, these only depend on b, a, and s). There is no mode with all currents having the same magnitude and this is generally true for all $N \geq 3$.

To obtain a feeling for how the $A_n^{\boldsymbol{\alpha}}$ values behave, consider the limit $b/s \gg 1$. Setting the current amplitude on the center nanotube to unity, it is found that the values of $A_n^{\boldsymbol{\alpha}}$ decrease from unity slowly as n increases. For example, for $b = 20\ \mu$m, $s = 2a = 1.763$ nm, and $N = 119$ nanotubes, more than half of the nanotubes have $A_n^{\boldsymbol{\alpha}} > 0.98$ and even the outermost nanotube has $A_N^{\boldsymbol{\alpha}} = 0.89$. More generally, for a given mode, the $A_n^{\boldsymbol{\alpha}}$ coefficients will decrease moving away from the center tube, with the rate of decrease depending on the geometry. For the fundamental mode, all $A_n^{\boldsymbol{\alpha}}$ have the same sign. In numerical experiments, it is found that often the simple approximation $A_n^{\boldsymbol{\alpha}} = 1$ for all n works fairly well, resulting in

$$L_{es}^{\boldsymbol{\alpha}} = L_{es} = \frac{\mu}{2\pi}\left(\ln\left(\frac{b}{a}\right) + 2\sum_{n=1}^{N-1/2}\ln\left(\frac{d_n}{ns}\right)\right) \tag{43}$$

$$C_{es}^{\boldsymbol{\alpha}} = C_{es} = \frac{2\pi\varepsilon}{\left(\ln\left(\frac{b}{a}\right) + 2\sum\limits_{n=1}^{N-1/2}\ln\left(\frac{d_n}{ns}\right)\right)}. \tag{44}$$

(some numerical comparisons are shown in Section IV). For large arrays, the advantage of (43) and (44) when used in (37) and (19), respectively, is that the inverse of a large matrix does not need to be computed, $\mathbf{C} = 2\pi\varepsilon\mathbf{P}^{-1}$, as in (17), nor do we need to determine the eigenvectors of a large matrix $\mathbf{P}$. The capacitance (44) is identical to the result in [6] in the limit that $N \longrightarrow \infty$, in which case,

$$C_{es} = \frac{2\pi\varepsilon}{\ln\left(\frac{s}{a}\frac{1}{\pi}\sinh\left(\frac{\pi b}{s}\right)\right)} \tag{45}$$

$$L_{es} = \frac{\mu}{2\pi}\ln\left(\frac{s}{a}\frac{1}{\pi}\sinh\left(\frac{\pi b}{s}\right)\right). \tag{46}$$

In a typical experimental situation, one would apply a common electrode to the nanotubes. For $\omega \longrightarrow 0$, C_{array} should provide the correct capacitance. However, one often works at

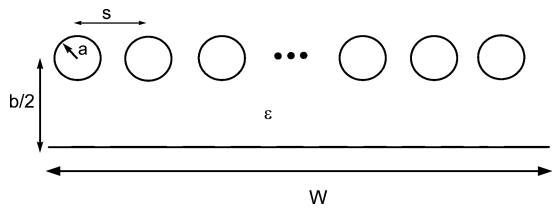

Fig. 4. Basic carbon-nanotube–ground-plane configuration.

$\omega > 0$ and measures S parameters of the device. In this case, we can not have a single mode propagating with all currents equal (because no mode exists such that $A_n^{\boldsymbol{\alpha}} = 1$ for all n, except for the case of two nanotubes). In general, the electrode would excite several modes on the array. Given that the lowest order mode generally carries most of the energy, the capacitance $C_{\text{array}}^{\boldsymbol{\alpha},\text{dyn}}$ with $\boldsymbol{\alpha}$ corresponding to the dominant mode should be the most accurate dynamic capacitance, in comparison with values extracted form S-parameter measurements. As described below, $C_{\text{array}}^{(1)}$ and $C_{\text{array}}^{(2)} = C_{\text{array}}^{\boldsymbol{\alpha},\text{dyn}}$ provide similar values.

D. Electrically Short Arrays

Finally, note that from the results above we have $\text{Im}\,(\beta) \sim \text{Re}\,(\beta)$ at low gigahertz frequencies, in which case all modes suffer high loss. As shown in [16], one obtains $\text{Im}\,(\beta) \ll \text{Re}\,(\beta)$ at several hundred gigahertz, leading to fairly low-loss propagation. Moreover, for the array case, we are often interested in arrays whose total width (horizontal direction in Fig. 1) W is much larger than the length of the nanotubes, l (see, e.g., [15], where $W = 110$ μm and $l = 1$ μm), and for active devices, where the nanotubes are electrically exceedingly short (e.g., at $f = 1$ GHz and $l = 1$ μm, $l/k \simeq 5 \times 10^{-8}$). Thus, we are often interested arrays consisting of a large number of electrically short nanotubes. For electrically short nanotubes, mode propagation aspects will be unimportant and the array would act like a lumped element having resistance (39), which can be quite small for large N. In this case, both capacitances $C_{\text{array}}^{(1)}$ and $C_{\text{array}}^{(2)}$ should provide values in reasonable agreement with measurement.

IV. Results

The basic geometry for the following results is shown in Fig. 4, where we will now consider the number of nanotubes above the ground plane to be N so that $s = (W - 2a)/(N - 1) \simeq W/(N - 1)$.

Since capacitance analysis is important in the design of carbon-nanotube field-effect transistors, we will first consider a typical transistor, a portion of which is shown in Fig. 5. The transistor consists of interdigitated source–drain fingers between which SWCNTs are grown, with gate fingers (the brighter narrower strips) above a portion of the tubes. Details of device performance have been presented elsewhere [17], [18]. We validate the presented analysis by comparison to measurements made on two structures similar to the one shown (for propriety reasons, we cannot show the exact structure). For these interdigitated structures, the sum of the length of the gate fingers (the sum of the vertical extensions of the narrow gate fingers shown in Fig. 5) corresponds to W in Fig. 4, which was

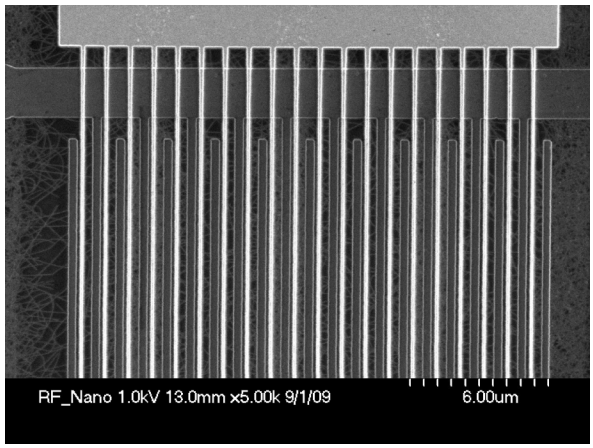

Fig. 5. Electron microscope image of a typical interdigitated transistor geometry. Source and drain fingers form the slightly wider, interdigitated pattern and narrower gate fingers lie above the source–drain plane. Carbon nanotubes run horizontally between the source and drain fingers.

TABLE I
Measured Capacitances and Theoretical Model

device	C_g (fF) measured	$C_{array}^{(2),\text{approx}} \times g_{eff}$ (fF) theory	$C^{\text{measured}}/C^{\text{theory}}$
1	265	177	1.50
2	395	254	1.56

400 μm for our devices. Gate-tube separation was 27.5 nm, and thus $b = 55$ nm and permittivity of the space between the gate and the nanotubes was $\varepsilon = 23\varepsilon_0$. Device 1 consisted of 2200 nanotubes ($s = 182$ nm) and Device 2 had 4000 nanotubes ($s = 100$ nm). Each tube had diameter 1.8 nm $\pm$0.3 nm as measured by AFM, consisting of a mix of 2/3 semiconducting and 1/3 metallic tubes.

Gate capacitance C_g was measured at a gate bias voltage of 2.5 V (approximately the maximum current bias point for the device), leading to $C_g = 416$ fF and $C_g = 552$ fF for Devices 1 and 2, respectively. From these values, we subtracted the corresponding values for the transistor metal structure without the presence of nanotubes; the pad/metallization capacitance was approximately 134 and 125 fF for Devices 1 and 2, respectively. This resulted in $C_g = 282$ fF and 427 fF for Devices 1 and 2, respectively. We then accounted for fringing capacitance (this is included in the model for the finite width W, but the model assumes infinite length nanotubes and thus does not include fringing effects in the axial direction due to the presence of finite length nanotubes), which was found to be C_g/α_f[19], where $\alpha_f = 1.066$ and 1.082 for Devices 1 and 2, respectively. This leads to the measured values in Table I. At the maximum bias, where most nanotubes should be turned on, we can model the tubes as $(13, 13)$ metallic nanotubes ($2a = 1.763$ nm). Table I also shows the computed values, where $C_{\text{array}}^{(2),\text{approx}} (= C_{\text{array}}^{\boldsymbol{\alpha},\text{dyn}})$ were evaluated using (19) and (32) with the approximation $A_n^{\boldsymbol{\alpha}} = 1$ for all n (this approximation is discussed below). Values computed using $C_{\text{array}}^{(2),\text{approx}}$ are in Farads/meter values and so these have been multiplied by the gate length, i.e., the length that electrons travel under the gate. This is nominally $g = 0.45$ μm and $g = 0.375$ μm for Devices 1 and 2, respectively; however, the nanotubes are not completely straight

and aligned perpendicular to the gate. Using a typical value of misalignment of 30° effectively lengthens the gate by about 15%, resulting in effective gate lengths of $g_{\text{eff}} = 0.52\ \mu$m and $g_{\text{eff}} = 0.43\ \mu$m for Devices 1 and 2, respectively. This also modifies the effective nanotube spacing to be the spacing s multiplied by g/g_{eff}.

Given the differences in the actual interdigitated geometry and the model, the agreement between measurement and theory in Table I is quite reasonable. The last column of Table I provides the ratio of measured to simulated capacitance. The similarity between the two ratios indicates that the model well accounts for the geometry of the structure (i.e., number of tubes, tube spacing, etc.); the factor of ~1.5 (ideally, this would be 1.0) is most likely due to the difference between measured and modeled geometry. Note that the assumption of the nanotube-gate geometry as a simple parallel-plate capacitor results in $C_{\text{pp}} = \varepsilon W g/(b/2) = 1333$ fF for Device 1 and 1111 for Device 2, which differs considerably from the measurement (in computing C_{pp}, we use the gate area Wg; if one used g_{eff}, then width is effectively decreased such that the gate area remains the same). Aside from the role of the quantum capacitance, the simple parallel-plate assumption fails because the tube density is fairly low (i.e., tube spacing s is relatively large compared with the spacing b), highlighting the need for a more rigorous theory. Furthermore, if we ignore the quantum capacitance, $C_{\text{array}}^{(2),\text{approx}} \times g = 338$ fF and 466 fF for Devices 1 and 2, respectively, so that the quantum capacitance of the tubes plays an important role in determining the value of C_{array}. The theory result is somewhat closer to the measured result if we ignore the quantum capacitance; we feel that this is a coincidence due to the difference between the actual and modeled structure, although we have no other measurements to compare with. Good agreement of our theoretical results with the result in [6] is described below.

As another check on the analysis, we look at the limit as the nanotube spacing becomes small. We consider $(13, 13)$ nanotubes with $b = 10$ nm and let the total width of the array be fixed at $W = 100$ nm. As the number of nanotubes N increases, s decreases (the nanotube density increases) and when $N = 57$, $s = 1.7857$ nm, which is the densest array possible. We first ignore the quantum capacitance ($C_q \to \infty$) and compare a dense array to the common parallel-plate capacitor result. In Fig. 6, the capacitance of the array is shown for an air dielectric as a function of spacing s. The level $C_{\text{pp},1}$ is the result from a simple parallel-plate model, $C_{\text{pp},1} = \varepsilon W/(b/2)$ (the plate-ground plane separation is $b/2$). Obviously, this value does not include fringing fields. The level $C_{\text{pp},2}$ is from a modified parallel-plate form $C_{\text{pp},2} = \varepsilon W/(b/2 + \delta)$, where $\delta = (s/\pi)\ln(2/2\pi a)$ is a correction factor to account for a wire grid model of each ground plate [20, (88)]. In that derivation, noninteracting infinite wire arrays form infinite plates; the correction factor δ is approximate, but helps to account for the fact that the plates are not solid conductors (although fringing is not accounted for). In Fig. 6, we only show the value of $C_{\text{pp},2}$ for $s/2a$ slightly larger than one since, although $C_{\text{pp},2}$ is a function of s, it is not expected to be accurate for large tube spacing. The result $C_{\text{array}}^{(2),\text{approx}}$ is evaluated from $C_{\text{array}}^{(2)}$ using (19) and (33) with the approximation $A_n^{\boldsymbol{\alpha}} = 1$ for all n [i.e., using (44)].

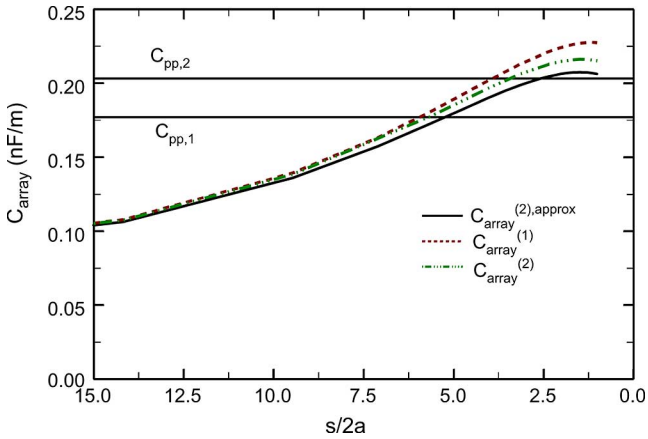

Fig. 6. Capacitance of an array of $(13, 13)$ nanotubes with $b = 10$ nm and fixed array width $W = 100$ nm, ignoring quantum capacitance. Nanotube spacing is $s = W/(N-1)$, where N is the number of nanotubes. C_{pp} are the parallel-plate capacitor results described in the text.

TABLE II
COMPARISON OF CAPACITANCE RESULTS (IN NANOFARADS) FOR $b = 10$ nm AND ARRAY WIDTH 1000 nm, WITHOUT INCLUDING THE QUANTUM CAPACITANCE

s (nm)	$C_{array}^{(2),\text{approx}}$	$C_{array}^{(2)}$	$C_{array}^{(1)}$	$C_{\text{Ref. [6]}}$
10	1.5142	1.5205	1.5311	1.4912
20	1.0130	1.0157	1.0192	0.9896
100	0.2505	0.2506	0.2506	0.2275

The result $C_{\text{array}}^{(2)}$ is the same as $C_{\text{array}}^{(2),\text{approx}}$, but evaluated using (33) with the $A_n^{\boldsymbol{\alpha}}$ values from the lowest order mode (and so this value should be more accurate than $C_{\text{array}}^{(2),\text{approx}}$). Also shown is the value $C_{\text{array}}^{(1)}$ (16) with $C_q \to \infty$ [i.e., (17)]. It can be seen that the three sets of results are in fairly good agreement (all values are with 10% of each other with $C_{\text{array}}^{(2)}$ and $C_{\text{array}}^{(1)}$ differing by 5%).

We now present some further simulations showing the comparison between $C_{\text{array}}^{(1,2)}$ and the effect of quantum capacitance on array capacitance. Using the same $(13, 13)$ carbon nanotubes and $b = 10$ nm, we fix the width of the array to be 1000 nm. Table II shows the capacitance values in nanofarads obtained from the various approaches for different nanotube spacing s, when the quantum capacitance is ignored. As discussed, $C_{\text{array}}^{(2),\text{approx}}$ is much easier to evaluate than $C_{\text{array}}^{(2)}$ since the latter requires determining the eigenvectors of a large matrix system, whereas the former is a simple closed-form expression. We also show the result of [6]; these values are for an infinite array and do not include fringing capacitance, and thus result in slightly lower values of capacitance.

Table III shows the same capacitance values as in Table II, when the calculation includes the quantum capacitance C_q. The difference with and without quantum capacitance is less than 10%. Since the electrostatic capacitance is in series with the quantum capacitance, for very small electrostatic capacitance values (say, moderately large spacing b), the quantum capacitance makes no difference, but for very small spacing between the nanotubes and the ground plane, the quantum capacitance can provide a very important contribution.

For the same structure as in the Tables II and III, in Fig. 7 we plot C_{array}/C_q for two different values of relative permit-

TABLE III
COMPARISON OF CAPACITANCE RESULTS (IN NANOFARADS) FOR $b = 10$ nm AND ARRAY WIDTH 1000 nm, INCLUDING QUANTUM CAPACITANCE C_q

s (nm)	$C_{array}^{(2),\text{approx}}$	$C_{array}^{(2)}$	$C_{array}^{(1)}$	$C_{\text{Ref. [6]}}$
10	1.4473	1.4531	1.4627	1.4264
20	0.9546	0.9570	0.9601	0.9338
100	0.2340	0.2341	0.2342	0.2139

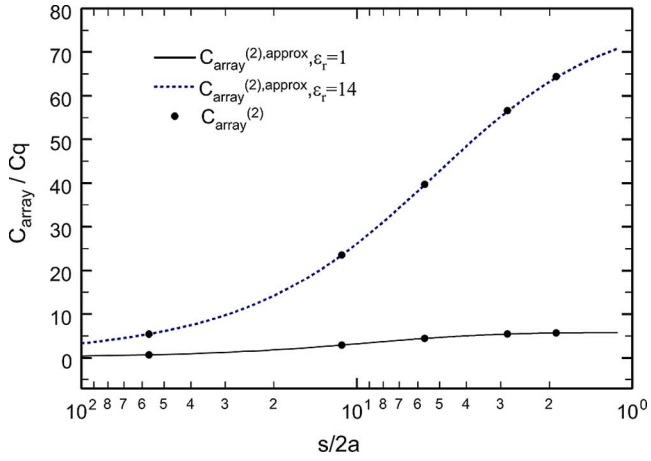

Fig. 7. C_{array}/C_q for two different values of relative permittivity, ε_r, for an array having $W = 1000$ nm.

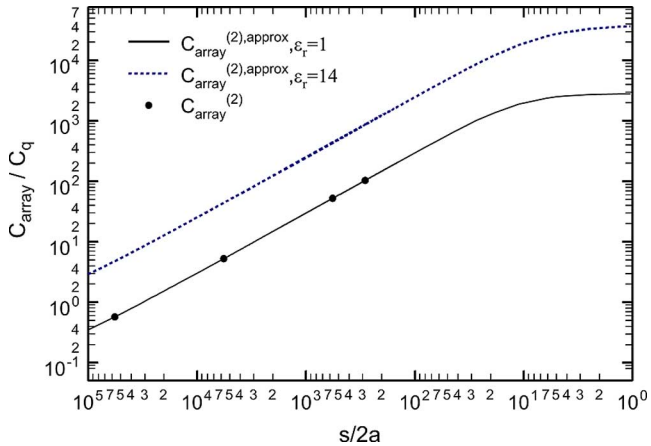

Fig. 8. Same as Fig. 7, except for $W = 1000$ μm.

tivity, ε_r. As before, $C_{\text{array}}^{(2),\text{approx}}$ is (19) with the approximation $A_n^{\boldsymbol{\alpha}} = 1$ for all n [i.e., using (44)] and $C_{\text{array}}^{(2)}$ is evaluated using (33) with the $A_n^{\boldsymbol{\alpha}}$ values from the lowest order mode. The difference in the results from each method is indistinguishable on the scale of the plots. The values of $C_{\text{array}}^{(1)}$ are not shown, but they are essentially the same as the results of $C_{\text{array}}^{(2)}$ or $C_{\text{array}}^{(2),\text{approx}}$. It is clear from the figure that for a dense array with a moderately large dielectric $C_{\text{array}}/C_q \gg 1$ is achievable, which is important in achieving linearity of carbon-nanotube field-effect transistors [21].

Now, for a much wider array having $W = 1000$ μm and $b = 20$ nm, Fig. 8 shows C_{array} versus the tube spacing. Large values of C_{array}/C_q can be achieved with a sufficiently dense array.

V. CONCLUSIONS

Electromagnetic properties of finite planar arrays of infinite-length SWCNTs have been studied using a Boltzmann's/Maxwell's equation formulation, which does not require as an initial assumption an equivalent transmission line model. Special emphasis has been placed on defining and obtaining the array capacitance and inductance. The formulation has been checked against measured results and results have been presented for dense arrays of nanotubes showing that it is possible to achieve $C_{\text{array}}/C_q \gg 1$, which is important in achieving linearity of carbon-nanotube field-effect transistors.

APPENDIX
TOTAL STATIC CAPACITANCE MATRIX FROM THOMAS–FERMI EQUATION

In this appendix, using a Thomas–Fermi model [22], we show that the total capacitance matrix in the static case is $\left[\mathbf{C}^{-1} - (C_q/2)^{-1}\,\mathbf{1}\right]$, where $\mathbf{C}$ is the classic electrostatic capacitance matrix. This is an alternative method that provides a check on the capacitance part of (11).

For a charge density in a free space, the electrostatic potential is

$$\phi(\mathbf{r}) = \int_{\Omega'} \frac{\rho(\mathbf{r}')}{4\pi\varepsilon_0 |\mathbf{r} - \mathbf{r}'|} d\Omega' \tag{47}$$

where Ω' is the support of the charge. For charge on a carbon nanotube, $\rho(\mathbf{r}) = \rho(z,\phi)\,\delta(r-a)$ so that

$$\begin{aligned} Q(z) &= \int_0^a \int_0^{2\pi} \rho(z,\phi)\,\delta(r-a)\,r d\phi dr \\ &= a\int_0^{2\pi} \rho(z,\phi)\,d\phi \\ &= 2\pi a \rho(z) \end{aligned} \tag{48}$$

assuming $\rho(z,\phi) = \rho(z)$, where $Q(z)$ is C/m and $\rho(z)$ is C/m^2. Then

$$\phi(\mathbf{r}) = \frac{1}{4\pi\varepsilon_0} \int_{-\infty}^{\infty} \int_{-\pi}^{\pi} \frac{1}{R} \frac{Q(z')}{2\pi} d\phi' dz' \tag{49}$$

where

$$R = \sqrt{2a^2(1 - \cos(\phi - \phi')) + (z - z')} \tag{50}$$

$$= \sqrt{(z-z')^2 + b_{11}^2}. \tag{51}$$

The number density of electrons is

$$n = 4\int_k f(E(k)) \frac{dk}{2\pi} = 4\frac{2k_F}{2\pi} \tag{52}$$

where f is the Fermi distribution and the factor of 4 comes from the spin and valley degeneracy. At absolute zero, the number density of electrons $n(z)$ is $4k_F/\pi$, and thus the Fermi wavenumber is $k_F(z) = \pi n(z)/4$

[23]. The equilibrium electron charge density is then $Q(z) = -en(z) = -e4k_F(z)/\pi$ and the Fermi momentum is $p_F(z) = \hbar k_F(z) = \hbar\pi|Q(z)|/4e$. The chemical potential is $\mu(z) = \pm\sqrt{(E_g/2)^2 + p_F^2(z)v_F^2}$ such that for metallic tubes

$$\mu(z) = p_F(z)v_F. \tag{53}$$

The electrochemical potential must be constant along the nanotube at equilibrium,

$$\mu(z) - e\phi(z) = 0 \tag{54}$$

which leads to

$$\left(\frac{\hbar\pi v_F Q(z)}{4e}\right) = \frac{e}{4\pi\varepsilon_0}\int_{-\infty}^{\infty}\int_{-\pi}^{\pi}\frac{1}{R}\frac{Q(z')}{2\pi}d\phi' dz' + e\phi_{\text{ext}}(z). \tag{55}$$

The generalization to two nanotubes is

$$\left(\frac{\hbar\pi v_F Q_1(z)}{4e}\right) = \frac{e}{4\pi\varepsilon_0}(I_{11} + I_{12}) + e\phi^1_{\text{ext}}(z) \tag{56}$$

$$\left(\frac{\hbar\pi v_F Q_2(z)}{4e}\right) = \frac{e}{4\pi\varepsilon_0}(I_{21} + I_{22}) + e\phi^2_{\text{ext}}(z) \tag{57}$$

for all $-\pi \le \phi \le \pi$, $-\infty < z < \infty$, where

$$I_{\alpha\beta} = \int_{-\infty}^{\infty}\int_{-\pi}^{\pi}\frac{Q_\beta(z')}{2\pi R_{\alpha\beta}}d\phi' dz'. \tag{58}$$

Invoking the translational invariance of the structure,

$$Q_\beta(z) = Q_\beta e^{-j\beta z} \quad \phi_{\text{ext}}(z) = \phi_{\text{ext}}e^{-j\beta z} \tag{59}$$

we have

$$\tilde{Q}Q_1 = Q_1 I_0(a_1\beta)K_0(a_1\beta) + Q_2 K_0(b_{12}\beta) + 2\pi\varepsilon_0\phi^1_{\text{ext}}(\beta) \tag{60}$$

$$\tilde{Q}Q_2 = Q_1 K_0(b_{21}\beta) + Q_2 I_0(a_2\beta)K_0(a_2\beta) + 2\pi\varepsilon_0\phi^2_{\text{ext}}(\beta) \tag{61}$$

where

$$\tilde{Q} = \frac{2\pi\varepsilon_0\hbar\pi v_F}{4e^2} = \frac{2\pi\varepsilon_0 h v_F}{8e^2} = \frac{2\pi\varepsilon_0}{C_q}$$

where I_0 and K_0 are the usual modified cylindrical Bessel functions. Note that Q contains all information about the nanotube's material properties.

The generalization to two parallel rows of nanotubes with each row consisting of N nanotubes is clear; we obtain

$$Q_n\left(\tilde{Q} - I_0(a\beta)K_0(a\beta)\right) - \sum_{m=1,m\neq n}^{2N} Q_m K_0(b_{nm}\beta) = 2\pi\varepsilon_0\phi^{\text{tube }n}_{\text{ext}} \tag{62}$$

$n = 1, 2, \ldots, 2N$, where b_{nm} is the center-to-center distance between nanotubes n and m and imposing odd symmetry in the vertical direction due to the ground plane and renumbering currents leads to

$$Q_n\left(\tilde{Q} - [I_0(a\beta)K_0(a\beta) - K_0(b\beta)]\right) - \sum_{m=1,3,5,\ldots,m\neq n}^{2N} Q_m\left(K_0(b_{n,m}\beta) - K_0(b_{n,m+1}\beta)\right) = 2\pi\varepsilon_0\phi^{\text{tube }n}_{\text{ext}} \tag{63}$$

for $n = 1, 3, 5, \ldots, 2N$. The small argument approximation leads to

$$Q_n\left(\ln\left(\frac{b}{a}\right) - \tilde{Q}\right) + \sum_{m=1,3,5,\ldots,m\neq n}^{2N} Q_m \ln\left(\frac{b_{n,m+1}}{b_{n,m}}\right) = -2\pi\varepsilon_0\phi^{\text{tube }n}_{\text{ext}} \tag{64}$$

for N nanotubes above a ground plane, $n = 1, 3, 5, \ldots, 2N$.

In matrix form, this can be written as

$$\mathbf{M}\rho = \left[\mathbf{P} - \tilde{Q}\mathbf{1}\right]\mathbf{Q} = \mathbf{F} \tag{65}$$

where $\mathbf{M}$ is an $N \times N$ matrix and $\mathbf{Q}$ and $\mathbf{F}$ are $N \times 1$ column vectors.

Defining $\mathbf{L} = \mu/\pi\mathbf{P}$, we then have

$$\left[\mathbf{L} - \frac{\mu}{\pi}\tilde{Q}\mathbf{1}\right]\mathbf{Q} = \frac{\mu}{\pi}\mathbf{F} \tag{66}$$

where $\tilde{Q} = 2\pi\varepsilon_0/C_q$. This can be written as

$$\left[\mathbf{C}^{-1} - \frac{2}{C_q}\mathbf{1}\right]\mathbf{Q} = \frac{1}{\pi\varepsilon}\mathbf{F} = -2\phi_{\text{ext}}. \tag{67}$$

In this static formulation, we obtain the quantum capacitance matrix $(C_q/2)^{-1}\mathbf{1}$, in agreement with the dynamic result (11).

ACKNOWLEDGMENT

The author would like to thank P. Burke, University of California at Irvine, and D. McCarthy, Air Force Research Laboratory, Rome, NY, for helpful discussions concerning this problem.

REFERENCES

[1] R. Saito, G. Dresselhaus, and M. S. Dresselhaus, *Physical Properties of Carbon Nanotubes*. London, U.K.: Imperial College Press, 2003.

[2] Z. Yao, C. L. Kane, and C. Dekker, "High-field electrical transport in single-wall carbon nanotubes," *Phys. Rev. Lett.*, vol. 84, pp. 2941–2944, 2000.

[3] C. Ryu, K.-W. Kwon, A. L. S. Loke, H. Lee, T. Nogami, V. M. Dubin, R. A. Kavari, G. W. Ray, and S. S. Wong, "Microstructure and reliability of copper interconnects," *IEEE Trans. Electron Devices*, vol. 46, no. 6, pp. 1113–1120, Jun. 1999.

[4] M. E. T. Molares, E. M. Höhberger, C. Schaeflein, R. H. Blick, R. Neumann, and C. Trautmann, "Electrical characterization of electrochemically grown single copper nanowires," *Appl. Phys. Lett.*, vol. 82, pp. 2139–2141, 2003.

[5] A. Weisshaar, H. Lan, and A. Luoh, "Accurate closed-form expressions for the frequency-dependent line parameters of on-chip interconnects on lossy silicon substrate," *IEEE Trans. Adv. Packag.*, vol. 25, no. 5, pp. 288–296, May 2002.

[6] Q. Cao, M. Xia, C. Kocabas, M. Shim, J. Rogers, and S. Rotkin, "Gate capacitance coupling of singled-walled carbon nanotube thin-film transistors," *Appl. Phys. Lett.*, vol. 90, 2007, Art. ID 023516.

[7] C. Kshirsagar, H. Li, T. E. Kopley, and K. Banerjee, "Accurate intrinsic gate capacitance model for carbon nanotube-array based FETs considering screening effect," *IEEE Electron. Device Lett.*, vol. 29, no. 11, pp. 1408–1411, Nov. 2008.

[8] G. W. Hanson, "A common electromagnetic framework for carbon nanotubes and solid nanowires—Spatially dispersive conductivity, generalized Ohm's law, distributed impedance and transmission line model," *IEEE Trans. Microw. Theory Tech.*, vol. 59, no. 1, pp. 9–20, Jan. 2011.

[9] C. R. Paul, *Analysis of Multiconductor Transmission Lines*. New York: Wiley, 2007.

[10] P. J. Burke, "An RF circuit model for carbon nanotubes," *IEEE Trans. Nanotechnol.*, vol. 2, no. 1, pp. 55–58, Mar. 2003.

[11] G. Y. Slepyan, S. A. Maksimenko, A. Lakhtakia, O. Yevtushenko, and A. V. Gusakov, "Electrodynamics of carbon nanotubes: Dynamic conductivity, impedance boundary conditions and surface wave propagation," *Phys. Rev. B, Condens. Matter*, vol. 60, pp. 17136–17149, Dec. 1999.

[12] G. Miano, C. Forestiere, A. Maffucci, S. A. Maksimenko, and G. Y. Slepyan, "Signal propagation in carbon nanotubes of arbitrary chirality," *IEEE Trans. Nanotechnol.*, vol. 10, no. 1, pp. 135–149, Jan. 2011.

[13] L. D. Landau, E. M. Lifshitz, and L. P. Pitaevskii, *Electrodynamics of Continuous Media*, 2nd ed. Amsterdam, The Netherlands: Elsevier, 1984.

[14] M. Krcmar, W. M. Saslow, and A. Zangwill, "Electrostatics of conducting nanocylinders," *J. Appl. Phys.*, vol. 93, pp. 3495–3500, 2003.

[15] C. Rutherglen, D. Jain, and P. J. Burke, "RF resistance and inductance of massively parallel single walled carbon nanotubes: Direct, broadband measurements and near perfect 50 ohm impedance matching," *Appl. Phys. Lett.*, vol. 93, 2008, Art. ID 083119.

[16] G. H. Hanson, "Current on an infinitely long carbon nanotube antenna excited by a gap generator," *IEEE Trans. Antennas Propag.*, vol. 54, no. 1, pp. 76–81, Jan. 2006.

[17] M. Schroter, S. Mothes, D. Wang, S. McKernan, P. Kolev, N. Samarakone, M. Bronikowski, Z. Yu, and P. Kempt, "A 0.4 μm CNTFET technology for RF applications," in *GomacTech*, 2011, pp. 367–370.

[18] M. Schroter, P. Kolev, D. Wang, M. Eron, S. Lin, N. Samarakone, M. Bronikowski, Z. Yu, P. Sampat, P. Syams, and S. McKernan, "A 4 wafer photostepper-based carbon nanotube FET technology for RF applications," presented at the IEEE MTT-S Int. Microw. Symp., 2011.

[19] M. Haferlach and M. Schroter, "Modeling of the gate capacitance of CNTFETs," RF Nano Corporation, Newport Beach, CA, Internal Rep., 2010.

[20] C. E. Baum, "Impedances and field distributions for parallel plate trsmmission line simulators," Kirtland AFB, Albuquerque, NM, Interaction Note 21 (Phillips Labor. Note Series), Jun. 1966 [Online]. Available: http://www.ece.unm.edu/summa/notes/Interaction.html

[21] J. E. Baumgardner, A. A. Pesetski, J. M. Murduck, J. X. Przybysz, J. D. Adam, and H. Zhang, "Inherent linearity in carbon nanotube field-effect transistors," *Appl. Phys. Lett.*, vol. 91, 2007, Art. ID 052107.

[22] E. G. Mishchenko and M. E. Raikh, "Electrostatics of straight and bent single-walled carbon nanotubes," *Phys. Rev. B, Condens. Matter*, vol. 74, 2006, Art. ID 155410.

[23] X. Zhou, J.-Y. Park, S. Huang, J. Liu, and P. L. McEuen, "Band structure, phonon scattering and the performance limit of single-walled carbon nanotube transistors," *Phys. Rev. Lett.*, vol. 95, 2005, Art. ID 146805:1–4.

George W. Hanson (S'85–M'91–SM'98–F'09) was born in Glen Ridge, NJ, in 1963. He received the B.S.E.E. degree from Lehigh University, Bethlehem, PA, in 1986, the M.S.E.E. degree from Southern Methodist University, Dallas, TX, in 1988, and the Ph.D. degree from Michigan State University, East Lansing, in 1991.

From 1986 to 1988, he was a Development Engineer with General Dynamics, Fort Worth, TX, where he was involved with radar simulators. From 1988 to 1991, he was a Research and Teaching Assistant with the Department of Electrical Engineering, Michigan State University. He is currently a Professor of electrical engineering and computer science with the University of Wisconsin–Milwaukee. He coauthored *Operator Theory for Electromagnetics: An Introduction* (Springer, 2002). He authored *Fundamentals of Nanoelectronics* (Prentice-Hall, 2007). His research interests include nanoelectromagnetics, mathematical methods in electromagnetics, electromagnetic wave phenomena in layered media, integrated transmission lines, waveguides, and antennas and leaky wave phenomena.

Dr. Hanson is a member of URSI Commission B and Sigma Xi and Eta Kappa Nu. He was an associate editor for the IEEE TRANSACTIONS ON ANTENNAS AND PROPAGATION (2002–2007). He was the recipient of the 2006 S. A. Schelkunoff Best Paper Award of the IEEE Antennas and Propagation Society.

Steffen McKernan received the B.S. degree in engineering physics from the University of California at Berkeley, in 1989, and the Ph.D. degree in physics from Princeton University, Princeton, NJ, in 1995. His doctoral research concerned low-dimensional electronic systems.

He is a founder of RF Nano Corporation, Newport Beach, CA, and is currently on their Board of Directors.

Dawei Wang received the B.S. degree in electronics and M.S. degree in electronic physics from Peking University, Beijing, China, in 1992 and 1995, respectively, and the Ph.D. degree from the University of California at Irvine, in 2005.

In 2006, he joined the RF Nano Corporation, Newport Beach, CA, where he has been involved with the research and development of carbon-nanotube RF transistors.